Princeton University

Department of Aerospace and Mechanical Sciences

PRELIMINARY DRAFT - FOR REVIEW PURPOSES ONLY

AN IN-FLIGHT SIMULATION OF APPROACH AND LANDING OF A STOL TRANSPORT WITH ADVERSE GROUND EFFECT

by

David R. Ellis
Princeton University

FINAL REPORT

Prepared by Princeton University
for Langley Research Center
NATIONAL AERONAUTICS AND SPACE ADMINISTRATION
Contract NAS1-11543

TABLE OF CONTENTS

AN IN-FLIGHT SIMULATION OF APPROACH AND LANDING OF A STOL TRANSPORT WITH ADVERSE GROUND EFFECT

by

David R. Ellis
Princeton University

SUMMARY

The results of an in-flight simulation program undertaken to study the problems of landing a representative STOL transport in the presence of adverse ground effects are presented. Landings from a 6^{o}, 70 kt approach were performed with variations in ground effect magnitude, ground effect lag, and thrust response. Other variations covered the effects of augmented lift response, SAS-failures, turbulence, segmented approach, and flare warning. In general, the basic STOL airplane required coordinated use of both stick and throttle for consistently acceptable landings, and the presence of adverse ground effects made the task significantly more difficult. Ground effect lag and good engine response gave noticeable improvement, as did augmented lift response.

INTRODUCTION

Wind tunnel tests and analysis indicate that powered-lift airplanes operated at high lift coefficients in close proximity to the ground will exhibit adverse ground effects – lift loss, drag reduction, and nose down pitching moment. The phenomenon appears to be common to all powered-lift concepts (References 1 and 2), and brings into question the ability of the pilot to perform landing maneuvers with desired consistency and accuracy.

This report presents the results of an in-flight simulation program undertaken to study the problems of landing a representative STOL transport (based on the EBF concept of Reference 3) in the presence of adverse ground effects.

The program was carried out in two stages, the first involving preparation and calibration of the simulator, and some 70 data landings which explored basic piloting problems for a three-engine thrust case. The second was more extensive - 340 data landings - with a broadened scope which concentrated effort on normal four engine operation and ground effects typical of a high wing EBF STOL. This second stage featured refinements in the ground effect simulation, including definition and cancellation of the basic simulator ground effect, and increased pitch control power for the cases with longitudinal SAS-off. (The latter step was taken to remedy a control authority limitation which in retrospect was felt to be unjustifiably low, and which heavily influenced the results.)

The bulk of the data presented are from the second stage of testing; the following subjects are covered in the results:

- Influence of ground effect magnitude
- Influence of ground effect lag
- Influence of thrust response lag
- Effects of augmented lift response (Z_{δ_s} and Z_{α})
- Effects of SAS failures
- Influence of turbulence
- Segmented approaches ($6^{\circ}/4^{\circ}$)
- Usefulness of simple flare warning

Both NASA and Princeton evaluation pilots participated in the program, with most of the data landings being performed by the contractor.

DESCRIPTION OF THE EXPERIMENT

In-flight Simulator. The in-flight simulator used is pictured in Figure 1. Appendix A contains a detailed description of its systems and operational features. For this experiment, it is sufficient to note that it is a "fly by wire" airplane with stability and control characteristics adjusted to match those of an EBF STOL transport design in an approach and landing configuration; the adverse ground effects associated with high lift coefficient operation were simulated by making appropriate changes in lift, drag, and pitching moment as functions of altitude measured with a radar altimeter.

Flight Pattern and Procedures. The flight pattern and simulated STOL runway are shown in Figures 2 and 3. The evaluation pilot normally was given control on the crosswind leg and after lining up with the runway tracked a glidepath defined by a precision optical approach aid. Following the flare and touchdown, control was assumed by the safety pilot who carried out any configuration changes called for and flew the airplane into position for the next run.

Most of the testing was done with a 6° glideslope and an approach speed of 70 knots, which gave a nominal descent rate of 12.6 ft/ sec (3.8 m/ sec). Some special runs were carried out on a two segment approach with upper and lower slopes of 6° and 4° respectively.

The STOL runway markings were based upon the criteria of Reference 4; the resulting location of the touchdown zone with respect to the glideslope was found to be satisfactory for landings from the normal 6° approach.

Data Collection. Time histories of control inputs and airplane motion variables were obtained by means of telemetry. The data sample shown as Figure 4 displays five channels which were of primary interest: altitude and altitude rate, obtained from the radar altimeter; pilot's stick and throttle inputs; and a touchdown indication from an accelerometer mounted on the main

landing gear strut (the spike produced by the landing impact is marked with a triangle.

The spike in the h and $\dot{h}$ ~~forces~~ traces about five seconds before touchdown was produced by a reflector positioned as shown in Figure 3; if the airplane is ~~properly positioned~~ on the glideslope at that point, the altimeter should indicate 40 ft.

The $\dot{h}$ trace shown has been smoothed with a filter having a 0.4 sec time constant, and this must be accounted for in determining touchdown sink rate.

Additional data were obtained in the form of pilot commentary and ratings. The familiar Cooper-Harper scale of Reference 5 was used.

TEST CONFIGURATIONS

Basic STOL Configuration. The simulation was based upon the externally-blown flap transport studied in Reference 3 . This was a high-wing, four-engine, T-tail configuration with the following general features:

Weight	244,660 N (55,000 lb)
Thrust-weight ratio (4-engines)	0.6
Wing loading	3590 N/m^2 (75 lb/ft^2)
Span	22.2m (73 ft)

For a 70 kt approach condition, the simulated longitudinal characteristics were as follows:

	SAS-Off	SAS-On
• Pitch Dynamics	Conventional,	θ, $\dot{\theta}$ Augmentation,
	ω_{sp} = 1 rad/sec	ω_{θ} = 1.5 rad/sec
	ζ_{sp} = 0.8	ζ_{θ} = 0.6
	ω_{p} = 0.22	No phugoid
	ζ_{p} = .001	
• Pitch Control	$\ddot{\theta}_{max}$ = 0.78 rad/sec^2	Attitude Command
		θ/δ_s = 1.6°/cm (4°/in.)
		Attitude Trim
		$\dot{\theta} \cong 2°$/sec
• $d\gamma/du$, (°/kt)	0.72 (Backside)	~0 (X_u Augmentation)
• Lift Response, Z_α/V	0.38 ft/sec^2/rad	0.38
n/α	1.4 g/rad	1.4

The corresponding lateral directional characteristics were:

• Yaw Control, $N_{\delta r}\delta r_{max}$	0.4 rad/ sec^2
• Roll Control, $L_{\delta a}\delta a_{max}$	0.5 rad/ sec^2
• Roll Mode Time Constant, τ_r	0.5 sec (p Augmentation)
• Dutch Roll Frequency, ω_d	1.0 rad/ sec
• Dutch Roll Damping Ratio, ζ_d	0.40 ($\dot{\psi}$ Augmentation)
• Spiral Mode	Slight Divergence
• Dihedral Effect, L_β	0.4 rad/ sec^2/ rad

A list of dimensional stability derivatives is given in Appendix B.

The cockpit controls were conventional stick, rudder pedals, and throttle, with no perceptable nonlinearities or breakout forces. Force gradients and maximum displacements were:

Control	Deflection	Gradient
Stick		
Pitch	19.8 cm (5.5 in.) aft 10.4 cm (4.0 in.) forward	7.9 N/ cm (4.5 lb/ in.)
Roll	±7.6 cm (±3.0 in.)	4.3 N/ cm (2.5 lb/ in.)
Pedals	±5.1 cm (±2.0 in.)	43 N/ cm (25 lb/ in.)
Throttle	0^o-60^o	Adjustable Friction

Instruments were arranged in a standard "T" layout.

Ground Effect Variation. Ground effect variations were based upon information derived from Reference 3, with later revisions suggested by the sponsor. The basic lift, drag, and pitching moment changes used in the experiment are shown in Figure 5. These are plotted for a particular out-of-ground-effect lift coefficient, $C_{L_\alpha} = 5$, and display a characteristic lift loss

(about 12% at touchdown), drag decrease, and nose down pitching moment as a function of wing height to wing span ratio, h/b.

The curves shown as solid lines in the figure were approximated for simulation purposes by straight line segments starting at h/b = 0.7; accounting for the differing geometries of the transport and the Navion (and considering the landing gear ground contact points to be superimposed for the two machines), this corresponded to a simulator wheel height of 12.2 m (40 ft).

In addition to the variation with altitude shown in Figure 5, the ground effects changed as a function of lift coefficient, becoming more pronounced as C_{L_∞} increased. The variation of lift loss with C_{L_∞} is shown in the upper part of Figure 6. In flight, the changes in C_{L_∞} are due to changes in angle of attack, and thrust, and the lower half of Figure 6 displays the combined effects of ground proximity, thrust variation, and angle of attack change on lift. Here each quadrilateral represents the conditions at a given height, h/b, with the small cross in the center denoting the lift for a combination of angle of attack and thrust which give the nominal test lift coefficient, $C_{L_\infty} = 4.53$ (corresponding to an approach speed $V_A = 70$ kt). The corners of the quadrilaterals represent the lift condition resulting from changing angle of attack by $\pm 1^\circ$ and thrust lever position by $\pm 13^\circ$. The general lowering of the small figures for successively smaller values of h/b is the direct effect of altitude; the apparent skewing, or rotation, represents the secondary decrease in effectiveness of angle of attack and thrust changes as the airplane approaches the ground.

In the simulation these ground effects were accounted for by driving the Navion flap according to

$$Z_{\delta t_N} \Delta\delta_{f_N} = \frac{\Delta h}{m_S}\left[\left(\frac{\partial Z}{\partial h}\right)_S + \left(\frac{\partial^2 Z}{\partial \alpha\, \partial h}\right)_S \Delta\alpha + \left(\frac{\partial^2 Z}{\partial \delta_t \partial h}\right)_S \Delta\delta_t\right]$$

to produce the same vertical acceleration that the STOL would experience with corresponding changes in altitude, angle of attack, and thrust lever position. Similar changes in drag and pitching moment ground effects take place as α and δ_t vary, and were handled in the same manner as lift variations; appropriate X-accelerations were produced by the simulator powerplant and pitching accelerations by the elevator. The procedures used to estimate the required derivatives and calibrate the system are covered in Reference 6.

The altitude measurement required for the simulation was done by means of a radar altimeter (Honeywell Model 7182) which is described in Reference 7.

The normal ground effects of the Navion airframe were canceled by use of radar altimeter signals to flap and elevator, the functions of altitude being determined by a combination of calculation (for lift) and flight measurement (pitching moment). Navion drag variations were not accounted for, since they appeared to produce no significant speed change during the abbreviated STOL flare. An in-flight calibration procedure consisting of steady, shallow approaches to ground contact was used to confirm that the simulator had essentially no response due to ground proximity. Further details of this procedure may be found in Reference 8.

Ground Effect Lag. The STOL ground effect functions discussed above do not take into account possible unsteady effects which could delay the onset of the force and moment changes. The experiments described in Reference 9 suggest that such effects could exist, although the results are difficult to interpret in a useful quantitative way.

Despite the lack of precise knowledge of the phenomenon, it seemed desirable to explore the influence of such lags on the landing maneuver, and several variations were simulated by passing the radar altitude signal through a first-order lag network. The particular cases tried had first order time constants, τ_h, of 0, 0.2, and 0.4 sec.

Thrust Response. The data available indicated that the EBF STOL would be operating with at least 50% of maximum thrust in the trimmed approach condition, in which case the engine response characteristics could be approximated as first-order lags without seriously compromising the simulation. This was particularly true if the intermediate thrust level exceeded 70%. A response lag of 0.4 sec was selected for the standard, or baseline, configuration; variations of zero, 0.25, and 0.6 sec were available as alternatives.

Strictly speaking, the stated lag applied not to the STOL engine response, but to the lift and moment responses to a thrust command. The simulated thrust, or X-force, response was further slowed by the natural lag of the Navion engine, but this is known to be shorter than 0.25 sec, and was felt not to be a significant factor because the predominant response to a thrust command in the simulated STOL airplane is a change in lift ($X_{\delta t} / Z_{\delta t} = -0.196$ in the approach and landing configuration).

Turbulence Simulation. The influence of atmospheric turbulence was studied by introducing filtered noise signals from an on-board tape recorder to the control surfaces in the manner described in Reference 10. Vertical gusts and side gusts with an RMS intensity of 1 m/ sec (3 ft/ sec) were simulated; fore-and-aft gust components were not accounted for.

Other Configuration Variables. The program included several other variations which are covered in appropriate detail in the section on results. They include

- Flare warning instrumentation
- Segmented glide slope
- SAS - failures
- Lift response augmentation through Z_{δ_s} or Z_{α}.

DISCUSSION OF RESULTS

Background. Before considering the results in detail, it is useful to have in mind the framework and constraints within which the evaluation pilots were operating:

- Operations were in day VFR conditions with precision optical approach guidance, and the pilot rating (or workload evaluation) sought was for that situation; comments on the possible influence of night or IFR operation or other factors were welcomed, but extrapolation of the rating was discouraged since such conditions were not actually simulated.
- Touchdowns were to be made in the marked 200 ft (60m) zone on the runway, but at a low sink rate if possible. Touchdown point precision within the zone was not to be emphasized at the expense of hard landings. Precise tracking of the 6^{o} optical guidance down to the point of flare initiation was encouraged.
- For purposes of judging adequacy of performance (which the pilot must do in order to use the rating system), the somewhat arbitrary concensus was that touchdown sink rates less than 3.5 ft/ sec (~1 m/ sec) were clearly satisfactory, and that 6.5 ft/ sec (~2 m/ sec) was marginally acceptable.
- The pilots could not expect conventional transport control techniques to yield acceptable landings; they were instructed to use any technique which would give consistent results, and then rate the task in terms of difficulty and workload.

Ground Effect Magnitude. The influence of ground effect magnitude is presented in Figure 7, where landing performance and pilot rating are shown for variations in lift ground effect, with and without longitudinal SAS. The

level of ground effect is noted in terms of $\Delta C_L / C_{L_\infty}$ for the nominal approach condition, $C_{L_\infty} = 4.53$; off-nominal values of angle of attack or thrust setting would vary the lift change as indicated in the preceding section on configurations. Data shown are for the "baseline" case with all engines operating, normal thrust response ($\tau_T = 0.4$ sec), no ground effect lag, and no simulated turbulence.

The general trend of piloting performance is for dispersion in both touchdown sink rate and touchdown distance to increase as the ground effect becomes more negative, although almost all of the landings were accomplished with less than 5 ft/ sec (1.5 m/ sec) vertical velocity and within the confines of the 200 ft (60 m) marked touchdown zone on the runway. For any one case, some of the dispersion might be attributed to atmospheric conditions (head or tailwind components of up to 5 kt were allowable during testing, as long as turbulence and shear were not factors), but the systematic degradation of pilot rating indicates increasing difficulty with the flare maneuver as the ground effect becomes adverse.

The results and the pilot commentary support the idea that technique and experience were critical factors in achieving consistently acceptable landings. The pilots quickly determined that a complete flare from the 6^o approach could not be accomplished with an angle of attack increase alone, even with the positive ground effect airplane, due to the low level of lift response ($Z_\alpha / V \cong 0.38$); this was aggravated in the SAS-off case by being well on the backside of the thrust-required curve. Thus some thrust application during the flare was required, but both timing and amount were critical because of the engine response lag and because there was sufficient thrust available to cause an overflare if the input was too large. The short duration of the flare maneuver together with the lag in response tended to make precise modulation impossible.

The technique of shallowing the descent with a partial power application and then holding attitude constant until touchdown was found to be feasible with positive and zero ground effect cases, although the thrust application was still somewhat critical. With negative ground effect this procedure almost invariably led to a build-up in sink rate and a shorter, harder touchdown than anticipated.

Some of these problems with control application are evident in the left half of Figure 8, which presents stick and throttle time histories for three successive landings. The configuration was SAS-off with negative ground effect. In this particular case only three-engine thrust was available but this was still sufficient to overflare the airplane if applied early; the main difference to the pilot was lowered throttle sensitivity compared to the four-engine machine. (This case is not covered in Figure 7.)

The use of both stick and throttle is apparent, but the timing of the thrust application is different for each run. An early power advance -- as much as 6 seconds prior to touchdown - clearly improves the touchdown sink rate results. A last-moment thrust command and aft stick movement may be noted, undoubtedly because both the lift loss and nose-down moments from the ground effect are most strongly apparent just prior to touchdown. An interesting small detail is the stick reversal at about one second prior to touchdown on the third landing (solid line), probably an attempt to counter the combined effects of maximum thrust and overrotation.

The right half of Figure 8 illustrates the technique which produced consistent results for one pilot. Here the configuration is SAS-on, although the same procedure was equally effective SAS-off; ground effect was negative, and four-engine thrust was simulated. Stick and thrust lever are both being used, but the power application is well in advance of touchdown and

clearly leads any large attitude command. According to this pilot the timing and magnitude of the power advance were based largely on experience with the configuration, being early enough to compensate for the slow engine response, and large enough to provide most of the lift increase needed in the flare without causing ballooning. Attitude (or angle of attack) was then modulated with the stick during the last stages of the landing to counter the ground effect and hold the sink rate to an acceptable value. Each landing was likely to be slightly different due to being high or low on the approach path, being fast or slow, or having a headwind or tailwind; however, the pitch response was fast enough to permit correction for the typical variations seen in the test program.

Although consistently acceptable touchdowns were obtained with this technique, the pilot rated it 4.0, commenting that although he felt the available controls were being used to best advantage, the task still demanded a good level of anticipation and coordination. He also pointed out that he was actively using all of the cues available in the VFR test situation, and that the results might degrade significantly for night or poor weather operations.

Ground Effect Lag. As noted in the section on configurations, there was interest in determining how a delay in build-up of the ground effect would influence the piloting problems in the flare maneuver. This was simulated by inserting a first-order lag in the output signal of the radar altimeter; τ_h is the time constant of that lagged signal.

The results of landings with two values of the ground effect lag are shown in Figure 9, compared with results for no lag. The basic airplane was the same in each case, with negative ground effect, SAS-on, and standard engine response, (τ_t = 0.4 sec).

Touchdown performance tended to improve somewhat even with the 0.2 sec lag, with a high incidence of landings at less than 3.5 ft/sec (1 m/sec) and in the middle of the landing zone. Further improvement was obtained with

the 0.4 sec lag, with results similar to those shown in Figure 7 for the positive ground effect case.

The pilot ratings improved by nearly one unit in going from no lag to a 0.4 sec lag, corresponding to an easing of difficulties with the flare. Even the small lag gave a noticeable lessening of the tendency for the airplanes to "fall out" at the last moment which normally led to increased sink rates and the need for rapid pitch adjustments. The landing technique with $\tau_h = 0.4$ sec could be changed to one of breaking the descent with thrust, followed by a modest attitude increase which was then held fairly constant to touchdown.

With lag present, the firmer touchdowns were due mainly to mishandling of the thrust addition. Flaring too high and floating long enough for the ground effect to build up to its full magnitude was not experienced, although it was expected to be a problem. The evaluation pilot for this series of tests was relatively experienced in the basic STOL airplane for all levels of ground effect, which may have been why this situation did not occur.

To summarize, on the basis of this limited investigation, even small delays in the buildup of negative ground effect appear to be noticeable ahd help to alleviate the landing problems.

Thrust response Lag. Because a timely thrust, and hence lift, addition was found to be necessary to flare the STOL airplane from a 6° approach, the simulated engine response lag was immediately picked out by the pilots as a factor which influenced the success of the flare maneuver. In particular, they commented that the basic lag, which was approximated as a first-order function with a time constant $\tau_t = 0.4$ sec, was long enough to interfere with their judgment of how much power to use in the initial stages of the flare, and to almost completely preclude precise thrust modulation in the last two or three seconds before touchdown. This led to the use of the technique discussed previously: an early, almost open-loop thrust command, with precise flight path adjustments through angle of attack.

The results of a series of runs in which the simulated thrust response was made both smaller and larger than the τ_t = 0.4 sec value are shown in Figure 10. The configuration was the basic SAS-on four-engine STOL with negative ground effect. For purposes of comparison, some runs done during the same period by the same pilot with the standard 0.4 sec thrust response are shown on the lower left plot.

With the response quickened to an equivalent first-order τ_t = 0.25 sec, a definite improvement was noted, both in performance and rating. For the first time the pilots felt they had a thrust/ lift control which was fast enough to allow modulation of sink rate during the flare, and in fact to permit some influence over touchdown point within the landing zone. The pilot rating improved from a deficient but acceptable 4.0 to the marginally-satisfactory level 3.5.

The improving trend continued with the thrust response lag entirely removed. The pilot on this abbreviated series felt that he now had the means to exercise consistent control over both sink rate and distance, through the thrust timing was still improtant, and the landing still demanded coordination of attitude and thrust. (The one firm, slightly short, landing shown was due to misjudgment in an attempt to land near the beginning of the touchdown zone.)

Making the thrust response slower than the basic value resulted in some degradation in rating, as shown in the lower right plot of Figure 10. The pilot commented that he was entirely committed to the early, near-open-loop thrust technique with that much lag (τ_t = 0.6 sec), and for the series of runs flown, the results were certainly acceptable. However, those particular landings were done consecutively during the latter part of one test period, and the pilot had developed a very good feel for the timing and amount of thrust needed; he doubted that he could perform as well if wind conditions changed, or if he had not had so much recent practice. On the other hand, he suggested that with the particular technique used, which did not demand quick thrust modulation, the thrust lag could possibly be somewhat longer yet without causing much degradation.

It is useful to note that all levels of thrust response tested were adequate for flying the precision optical approach, at least in smooth air.

Augmented Lift Response. The basic STOL airplane with its low lift response to angle of attack ($Z_\alpha / V = .38$) could not be adequately flared from a 6° approach with elevator alone, and required a relatively difficult coordination of stick and throttle for consistently acceptable landings. A brief series of runs was undertaken with augmented lift response to determine what benefits, if any, would result from allowing the pilot to use a more conventional flare technique.

Two different methods of augmenting the lift response were tried: a lift command directly from the pilot's stick (Z_{δ_s}), and an increased angle of attack response (Z_α). The results of a few trials with these systems in operation are shown in Figure 11. The basic configuration was SAS-on, four-engine thrust with standard 0.4 sec response, and negative ground effect. The shaded areas in the figures represent the envelope of results obtained without lift augmentation.

Although there are too few data points to make firm conclusions, the trend is toward definite improvement in both performance and pilot rating with even relatively small levels of augmentation. In the case of the direct interconnect between stick and lift, the pilot appreciated the almost direct control over sink rate. As in the case of improved thrust response, he could begin to be concerned over which half of the landing zone to use. A rating change from 3.5 to 2.5 was obtainable (note that a 0.2 sec ground effect lag was present for these runs), for favorable levels of Z_{δ_s}: a too-sensitive control caused a return to the original 3.5 rating.

Similar improvement was noted for straight Z_α augmentation on the basic airplane with no ground effect lag. The pilot felt that with practice he might be able to dispense entirely with a thrust advance, and have consistently satisfactory touchdowns in mid-zone. Even with a brief exposure, however, the extra lift response was confidence-inspiring.

SAS-Failures. Except for the SAS-off data shown in the section on the influence of ground effect magnitude, the results discussed thus far have been for the fully augmented STOL. A brief series of special runs was made to explore the influence of selective failures in the SAS system, with the results shown in Figure 12. Negative ground effect (no lag) and standard four-engine response are common to all of the points shown. The shaded area is an envelope of normal SAS-on landings, with a pilot rating of 4.0.

As noted on the figure, separate attitude hold and pitch damper failures caused no significant change in landing performance, but degraded the rating to 4.5 in each case. In the case of attitude-hold failure, the pitch damping was still sufficient to permit manual attitude control; for the damper failure case, the attitude hold still provided basic stabilization and the pilot apparently could cope with the reduced damping.

Autothrottle failure was of little consequence, probably because in the simulation a strong frontside characteristic was not provided (with autothrottle on, $d\gamma/dV \cong 0$), and the pilots were already accustomed to controlling glide path with thrust and speed with attitude; this was the required technique with autothrottle off. The abbreviated nature of the flare, along with the forward component of thrust accompanying the required throttle advance apparently prevented the backside characteristic from influencing the landing itself.

Influence of Turbulence. The influence of atmospheric disturbances was explored with a short series of special runs using simulated turbulence in the manner discussed in the section on experimental procedure. As noted there, a vertical and side gust field with an RMS velocity $\sigma_w = \sigma_v = 3$ ft/sec ($\sim$ 1 m/sec) was used. The pilot rating results may be summarized as follows for the baseline STOL machine with negative ground effect (no lag), and standard four-engine thrust with $\tau_t = 0.4$ sec:

Configuration	Pilot Rating In Turb.	No Turb.
SAS-On	5.5-6.5	4
SAS-Off	6.5-7	4.5
Pitch Damper Failed	7	5

Although it was generally possible to maneuver the airplane into the vicinity of the touchdown zone (a landing data point for the damper-failed case is shown on Figure 12), the ratings indicate a high degree of apprehension over the effects of the gusts during the flare. With the normal thrust response lag and lift response, the pilots felt that they did not have enough control over the higher frequency heave excursions to prevent being dropped onto the runway prematurely, or ballooned upward with subsequent recovery problems. They also noted that the overall physical workload was very high, especially with the pitch damper failed or SAS-off.

These findings should be qualified by noting that the simulation was incorrect in not diminishing the heave gusts as a function of altitude near the ground, and in not providing a simulation of the fore-and-aft gust component. In a way, the two deficiencies tend to compensate for one another close to the ground, since in actual practice the u-gusts remain to upset the airplane while the w-gusts diminish in magnitude; however, the disturbance inputs to the airplane are not the same for the two gust components, so the effect achieved in this simulation is not realistic.

Despite the deficiencies in the simulation, however, the results confirm that gust sensitivity is an extremely important consideration for STOL landing operations.

Segmented Approaches. A flare initiated directly from the 6° approach impressed some of the pilots as being an unnecessarily abrupt maneuver, and they indicated that they would feel considerably more confortable with a shallower stabilized final descent. This led to trials with a $6^{\circ}/4^{\circ}$ segmented

approach, with separate optical guidance provided for each angle as shown in Figure 13.

The landing performance results are shown in Figure 14; the airplane configuration was SAS-on, negative ground effect, with standard four-engine thrust (τ_t = 0.4 sec). During some of the landings the 0.2 sec ground effect lag was present, and these runs are indicated by solid symbols. Data points for several glide slope intersection heights are shown, ranging from $h_I = \infty$ (straight 4^o approach) to a close-in h_I = 50 ft (15 m). For the latter case the distance from the glide slope "corner" to the touchdown zone threshold was about 750 ft (230 m), or a little over six seconds at the nominal 70 kt approach speed.

The landing performance is seen to be uniformly good, the concentration toward the end of the zone being at least partly due to the fact that the guidance light bars were not moved away from the touchdown zone to compensate for the shallower approach.

The segmented approach itself posed no problems, even for the close-in intersect cases, but opinion was divided over whether or not the shallow final segment made the landing easier. The pilot with the most experience with 6^o approaches (more than 200 landings) felt that there was no significant improvement; other pilots with less than six-degree approach experience with this type of airplane felt more confident of making consistently acceptable landings.

Flare Warning. The necessity for a thrust addition to help flare the simulated STOL airplane, and the critical timing involved, have been mentioned repeatedly. This has led to simulator studies of flare-director concepts (Reference 11), and in the case of the present program, to an experiment in providing simple cueing to the pilot in the form of a flare imminence indicator.

The scheme tried, shown in Figure 15, consisted of a meter on the glare shield, close to the pilot's line of sight, driven by the radar altimeter

signal. The meter needle started a downward motion of a selectable altitude h, and hit the bottom stop at h_2 = 40 ft (12 m), the average altitude at which the pilots tended to initiate a thrust advance for a flare from a 6° approach. A few trials indicated that h_1 = 80 ft (24 m) gave a suitable time (approximately 3 seconds) and altitude increment for the pilot to be warned of the impending flare maneuver.

Results with and without the flare warning are shown in Figure 16 for the SAS-on, negative ground effect, four-engine (τ_t = 0.4 sec) airplane. No significant improvement in performance was noted, except possibly for less tendency to undershoot, which also could be attributed to more pilot experience with the machine at this stage of the program.

The pilots who tried the device were not enthused, claiming that it was distracting to have to focus their attention inside the cockpit at such a late stage of the approach, and that given the usual variations in speed and position at the flare initiation point, the information given by the meter was not very helpful. In particular, they still had no guidance other than their own judgment as to the amount of thrust advance needed, a factor equal in importance to the timing of the action.

Although this particular device proved not to be effective, the pilots stressed the desirability of some sort of flare director instrumentation which would be usable while looking outside, and which would help with thrust management throughout the approach, flare, and touchdown. As flown, the task was demanding even under calm, daylight conditions, with a pilot practiced and proficient in the airplane; the possibilities for degradation seemed obvious.

CONCLUSIONS

This report presents results of an in-flight investigation of piloting problems involved in landing a simulated powered-lift STOL transport exhibiting the form of ground effects associated with high-lift coefficient operation. Operations were in daylight, VFR conditions, using precision optical approach guidance. The majority of the landings were performed out of a 6°, 70 kt approach, with little or no wind or turbulence. Simulated turbulence was introduced on selected runs to determine its influence. Pilots were instructed to land within a marked touchdown zone, but at as low a sink rate as possible.

The following conclusions are based upon consideration of both landing performance measurements and pilot assessments:

- The basic STOL configuration required both a thrust advance and an angle of attack increase to flare to a low sink rate at touchdown; experience and technique are major factors in obtaining consistent, satisfactory results.
- The presence of adverse ground effect, particularly lift loss, clearly contributes to piloting difficulties, and accentuates other airplane deficiencies such as low Z_{α} and poor thrust response.
- Even small lags in the onset of lift loss ease the landing task.
- Fast engine response (that is, $\tau_t < 0.4$ sec) is beneficial, resulting in improved touchdown performance and pilot confidence.
- Augmenting the lift response with either Z_{δ} or Z_{α} interconnects is beneficial, allowing more conventional piloting technique and making the thrust increase in the flare less critical.

- The presence of turbulence - like disturbances caused a marked increase in workload and erosion of pilot confidence, particularly with a failed pitch damper.
- No clear advantage could be seen in a small sampling of $6^{\circ}/4^{\circ}$ segmented approaches, although some pilots felt more comfortable flaring from the shallower final segment.
- Simple flare warning in the form of an altitude cue is of little help in the landing maneuver; guidance as to the magnitude as well as the timing of the thrust increase is needed.

REFERENCES

1. Vogler, R. D. and Turner, T.R.: Wind Tunnel Investigation at Low Speeds to Determine Flow Field Characteristics and Ground Influence on a Model With Jet-Augmented Flaps. NASA TN 4116, 1957.

2. Gratzer, L. B. and Mahal, A. S.: Ground Effects in STOL Operations. AIAA Paper No. 71-579, June 1971.

3. Vogler, R. D.: Wind Tunnel Investigation of a Four-Engine Externally Blowing Jet-Flap STOL Airplane Model. NASA TND-7034, 1970.

4. Anon.: Planning and Design Criteria for Metropolitan STOL Ports, Federal Aviation Administration, Advisory Circular AC No. 150/5300-8, 5 November 1970.

5. Harper, R. P., Jr. and Cooper, G. E.: The Use of Pilot Rating in the Evaluation of Aircraft Handling Qualities. NASA TND-5153, April 1969.

6. Kline, G. F. and Hughes, F. F., Jr.: In-Flight Simulation of the Longitudinal Characteristics, Including Adverse Ground Effect, of a Heavy Transport STOL Aircraft. Princeton University Report No. 998T. August 1971.

7. Anon.: Evaluation of Honeywell Model 7182 Radar Altimeter. FAA Report RD-64-95, June 1964.

8. Seckel, E.: The Landing Flare: An Analysis and Flight Test Investigation. NASA CR-2517, May 1975.

9. Turner, T. T.: Ground Influence on a Model Airfoil With a Jet-Augmented Flap as Determined by Two Techniques. NASA TND-658, February 1961.

10. Franklin, J. A.: Turbulence and Longitudinal Flying Qualities. NASA CR-1821, July 1971.

11. Middleton, D. B.: Analysis of a Flare-Director Concept for an Externally Blown Flap STOL Aircraft. NASA TND-7760, November 1974.

APPENDIX A

THE IN-FLIGHT SIMULATOR

GENERAL DESCRIPTION

The In-flight Simulator is based upon a modified North American Navion airframe; the power plant is a Teledyne-Continental IO-520B engine of 212.6 kilowatts (285 hp) driving a McCauley constant speed propeller. Gross weight has been increased from the original 12230 to 14010 N(2570 to 3150 lb).

Several significant airframe modifications were made to improve the research capability of the machine:

The flap hinging and actuation were changed to allow up, as well as down, deflection over a ±30 deg range, resulting in increased lift modulation authority and smaller drag changes compared to the previous 0-40 deg down-only flap. Aerodynamics of the basic airframe and of this flap arrangement were explored in the full-scale wind tunnel tests reported in References A1 and A2.

The normal Navion main landing gear struts were replaced with those from a Camair twin (Navion conversion with nearly 40% increase in gross weight). Drop tests were conducted to optimize oleo strut inflation and orifice size, the final results indicating that the landing sink rate may be as high as 3.8 m/s (12.5 ft/s before permanent set will occur in the main gear or attaching structure. The original Navion nose gear strut was retained, but adjacent attachment fittings and structure were strengthened.

Other changes included redesign and relocation of the instrument panel, and incorporation of a single rear seat arrangement in place of the former bench seat in order to accommodate electronics and instrumentation equipment.

VARIABLE RESPONSE CONTROL SYSTEM

The in-flight simulator utilizes what is now commonly known as a "fly-by-wire" control system, that is, power-actuated control surfaces commanded by electrical signals. The signals come from the various cockpit controllers and motion sensors, and when appropriately processed and summed, provide a net signal to each servo-actuator, and, hence, an airplane response of a particular character and magnitude. In this case, the servos are hydraulic, supplied by an engine-driven hydraulic pump delivering about .03 m^3/ min at 5 x 10^6 N/ m^2 (9 gpm at 725 psi pressure).

Independent control over the three angular and two of the three linear degrees of freedom is provided for - the missing one being sideways motion.

MOMENT CONTROLS - Control over pitching, rolling, and yawing are through conventional elevator, aileron, and rudder control surfaces. The full authority (that is, maximum travel) of each surface is available, and the maximum deflection rate in each case is about 70 deg/ s. At a typical low operating speed of 70 knots, the available control powers are, respectively

Pitch: ±4.4 rad/ s^2 (from trim)

Roll: ±4.1 rad/ s^2

Yaw: ±1.3 rad/ s^2

The presently available inputs to each of these controls are shown in Table A1.

NORMAL FORCE CONTROL - Independent control over normal acceleratio.. is exercised through the Navion flap, modified to deflect up, as well as down, through a ±30 deg range. The upward motion provides increased lift modulation authority and tends to minimize the problems of drag and angle of zero lift changes.

TABLE A1

INPUTS TO MOMENT CONTROLS

Channel	Input	Function Varied
Pitch	Control column displacement	Control sensitivity
	Thrust lever	Simulated moment due to thrust
	Column thumbwheel	Simulated DLC moment
	Radar altitude	Ground effect moment
	Airspeed	Speed stability
	Angle of attack	Static stability
	Pitch attitude	Attitude hold sensitivity
	Pitch rate	Pitch damping
	Flap angle	Trim change from flap
	Flap rate	Moment from flap rate (approximate $M_{\dot{\alpha}}$)
	Integral of column displacement	Rate command gain
	Simulated turbulence	Turbulence response
Roll	Wheel displacement	Control sensitivity
	Sideslip	Dihedral effect
	Roll rate	Roll damping
	Yaw rate	Roll due to yaw rate
	Rudder pedal displacement	Roll due to rudder
	Simulated turbulence	Turbulence response
Yaw	Rudder pedal displacement	Control sensitivity
	Sideslip	Directional stability
	Yaw rate	Yaw damping
	Roll rate	Yaw due to roll rate
	Wheel displacement	Yaw due to aileron
	Simulated turbulence	Turbulence response

Actuation is hydraulic, with a maximum available surface rate of 110 deg/s. At 70 knots, the available authority is slightly more than ±0.5g.

Inputs presently available are shown in Table A2.

THRUST CONTROL - Thrust/drag modulation is by direct control of the engine throttle with an electrohydraulic servoactuator. At maximum continuous power the rate of climb is about 1000 ft/min (300 m/min); the maximum descent angle with throttle closed and V = 70 kt is $\gamma \cong -9^{o}$.

Inputs to the thrust/drag modulation system are shown in Table A3.

INTERCONNECTS - It may be noted in the lists of inputs for the system (Tables A1-A3) that several coupling functions are provided. For some experiments, it is desirable to remove interacting effects in the basic airframe: lift and moment changes from thrust may be eliminated with interconnects between the throttle actuator and the flap and elevator; and pitching moments due to flap angle and flap rate are countered with inputs to the elevator.

Simulated interacting effects are handled by using inputs from the various cockpit controllers: pitching moments and lift changes due to power are provided by interconnecting the elevator and the flap with the thrust lever (M_{δ_T}, L_{δ_T}); and lift and drag changes due to pitch controller displacement are represented in L_{δ_s} and D_{δ_s}. Other controllers may be similarly interconnected.

TABLE A2

INPUTS TO NORMAL FORCE CONTROL

Input	Function Varied
Control column displacement	Lift due to control (simulates elevator lift, or direct lift control integrated with column)
Thrust lever displacement	Lift due to thrust, direct lift control integrated with throttle
Column thumbwheel	Separate direct lift control
Radar altitude	Ground effect lift; wind gradients
Airspeed	Lift change with speed
Angle of attack	Lift response to angle of attack
Simulated turbulence	Turbulence response

TABLE A3

INPUTS TO THRUST/DRAG MODULATION SYSTEM

Input	Function Varied
Control column displacement	Drag due to control (simulated control surface drag; drag due to direct lift controls integrated with column)
Thrust lever displacement	Thrust command/throttle sensitivity
Column thumbwheel	Drag change due to direct lift control (separate controller)
Radar altitude	Ground effect drag change; wind gradients
Airspeed	Drag change with speed
Angle of attack	Drag change with angle of attack

SAFETY CONSIDERATIONS

By its very nature, landing research involves repeated exposure to minimum-speed, low-controllability situations, so special consideration was given to providing sufficient airframe strength and simulation system reliability to make the risk of damage from occasional hard touchdowns or control system failures acceptably low. The matter of strengthened landing gear was mentioned in an earlier section; the control system aspects will be discussed here.

SAFETY PILOT FUNCTION - Fundamental to the operation of an in-flight simulator is the concept that a safety pilot will continually follow the movements of the basic airplane controls, monitor the systems and the flight path, and be ready to disengage or override the evaluation pilot in case of a malfunction or unsafe condition. For disengaging, a disconnect switch on the control wheel is the primary cutout, with the main electrical and hydraulic controls providing secondary means of deactivating the system.

Manual override of the hydraulic servoactuators is possible for all controls except the flap. The force required is set through an adjustable poppet valve on each servo - 178N (40 lb) being typical.

Warning of system failures is provided by a flashing master warning light on the upper edge of the instrument panel in front of the safety pilot, with individual channel disengage warnings slightly lower and to the right.

REDUNDANT CONTROL CHANNELS - The elevator and aileron systems incorporate redundant control channels. The philosophy here is that hard-over control inputs resulting from system failures are particularly dangerous in this low-speed, low-altitude situation, and should be guarded against if possible. With the redundant channels, any substantial error between the commanded and actual control position is detected, and a switch-over to a second servo is made. The evaluation pilot retains control during

this process, but all inputs to the switched channel, except those from the control column, are eliminated, thus reducing the possibility that a defective transducer or signal path is causing the problem. Redundant sensors for the control input signal are incorporated; the other transducers are not duplicated. The fact that a channel has switched to the secondary servo is communicated to the safety pilot by the aforementioned warning lights, and he can then disengage the system and assume control.

The elevator is clearly critical with regard to failures which result in sudden full deflection, with the ailerons only slightly less so. Redundancy was not incorporated in the rudder or propeller pitch channels, because inadvertent disengages were felt to be less critical, and, since he follows pedal motions continuously, the safety pilot can very effectively override large-deflection failures. The flap channel was not duplicated because most failure modes are not hazardous - the surface trails aerodynamically at a 10 deg down position, and upon disengage, its return to this position from up-deflections is rapid. Down-flap deflections clearly pose no safety problem; up-flap hardovers could be hazardous due to the large lift loss, but this has proved to be a failure mode so instantly recognizable by the safety pilot that a disengage (with subsequent down-float of the flap) can be effected with very small altitude loss.

WAVEOFF AUTOMATION - To aid the safety pilot in recovering from an excessive sink rate situation, an "abort mode" system disengage can be used. Activated by pressing the disengage thumb switch, the flap travels at maximum rate to a 20 deg down position and power is automatically advanced to a climb setting; primary control reverts to the safety pilot. Using this system, recovery from a 70 kt, 6 deg approach (sink rate of 3.8 m/s or 12.5 ft/s) with a simulated up-flap failure can be made with less than 3 m (10 ft) altitude loss.

COCKPIT AND EVALUATION PILOT CONTROLS

The left seat is occupied by the safety pilot who operates the normal Navion wheel and rudder and the powerplant controls. Simulation system controls occupy the overhead and lower consoles.

The evaluation pilot is seated on the right and provided with a standard flight instrument layout and conventional stick, rudder, and throttle controls. Linear force gradients with no perceptable nonlinearities are incorporated. The gradients are ground adjustable by replacing springs. The values shown in Table A4 are currently being used.

TABLE A4

CURRENT VALUES FOR LINEAR FORCE GRADIENTS

Control	Force Gradient	Travel
Pitch stick	7.9N/ cm (4.5 lb/ in.)	10.4 cm forward (4.0 in.) 19.8 cm aft (5.5 in.)
Roll stick	4.3N/ cm (2.5 lb/ in.)	±7.6 cm (±3.0 in.)
Pedal	44N/ cm (25 lb/ in.)	±5.1 cm (±2.0 in.)
Throttle	Adjustable friction	60°

Note: Three-axis trimming is provided.

Special controls presently installed include the following:

1. Direct Lift: Thumbwheel separate controller; integrated with pitch column; integrated with throttle. Adjustable moment and drag interconnects are available.
2. Pitch attitude command proportional to column displacement, with trimmable attitude hold.

Attitude hold may also be selected with any of the direct lift systems engaged.

DATA ACQUISITION

Data acquisition is through telemetry, with 43 channels available. Airframe motion parameters (linear accelerations, angular rates, attitude, and heading), control inputs, and performance measures, such as localizer and glide-slope deviation, are normally recorded. Altitude and altitude rate are available from the radar altimeter.

Correlation of touchdown time with the other parameters is obtained through a recording of fore-and-aft acceleration of the main landing gear strut; wheel spinup loads produce enough strut motion to mark even very smooth landings.

REFERENCES

A1. Shivers, J. P., Fink, M. P., and Ware, G. M., "Full-Scale Wind-Tunnel Investigation of the Static Longitudinal and Lateral Characteristics of a Light Single-Engine Low-Wing Airplane," NASA TND-5857, June 1970.

A2. Seckel, E. and Morris, J. J., "Full-Scale Wind Tunnel Tests of a Low-Wing, Single-Engine, Light Plane with Positive and Negative Propeller Thrust and Up and Down Flap Deflection," NASA CR-1783 and Princeton University Report 922, August 1971.

APPENDIX B

STOL Longitudinal Derivatives

$\frac{Z_\alpha}{V}$ - 0.38 m/ sec^2/ rad per m/ sec (ft/ sec^2/ rad per ft/ sec)

X_α - 6.53 m/ sec^2 per rad (21.4 ft/ sec^2 per rad)

X_u - .054 m/ sec^2 per m/ sec (ft/ sec^2 per m/ sec)

M_v -.0108 rad/sec^2 per m/ sec (-.0033 rad/ sec^2 per ft/ sec)

M_α -.60 rad/ sec^3 per radian

$M_{\dot{\alpha}}$ -.45 rad/ sec^2 per rad/ sec

$M_{\dot{\theta}}$ -.77 rad/ sec^2 per rad/ sec

$\frac{Z_u}{V}$ -.0151 m/ sec^2/ m/ sec per m/ sec (.004602 ft/ sec^2/ rad per ft/ sec)

Z_{δ_t} -.0861 m/ sec^2 per degree (.2825 ft/ sec^2 per degree)

X_{δ_t} .0169 m/ sec^2 per degree (-.05537 ft/ sec^2 per degree)

$M_{\dot{\delta}_t}$ -.00192 rad/ sec^2 per degree

M_{δ_s} -.056 rad/ sec^2 per cm (-.142 rad/ sec^2 per inch)

STOL Lateral-Directional Derivatives

L_r	0.25 rad/ sec^2 per rad/ sec
L_β	-0.40 rad/ sec^2 per radian
L_p	-1.9708 rad/ sec^2 per rad/ sec
L_{δ_a}	.05 rad/ sec^2 per cm (0.13 rad/ sec^2 per inch)
N_r	-0.7027 rad/ sec^2 per rad/ sec
N_β	0.8681 rad/ sec^2 per radian
N_p	-0.04 rad/ sec^2 per rad/ sec
$\frac{Y_\beta}{V}$	-0.135 m/ sec^2/rad per m/ sec (ft/ sec^2/rad per ft/ sec)

FIGURE 1. IN-FLIGHT SIMULATOR

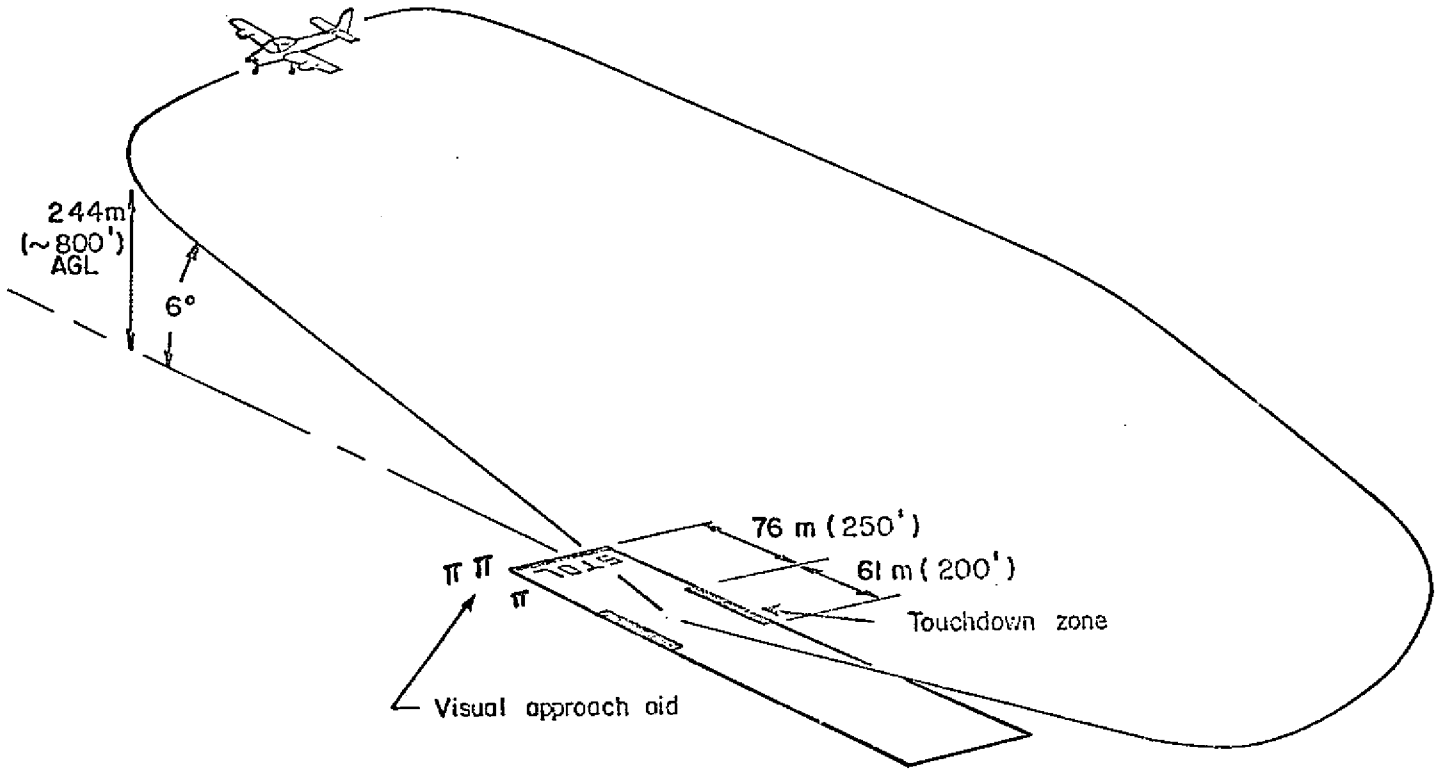

FIGURE 2. SIMULATED STOL RUNWAY AND FLIGHT PATTERN

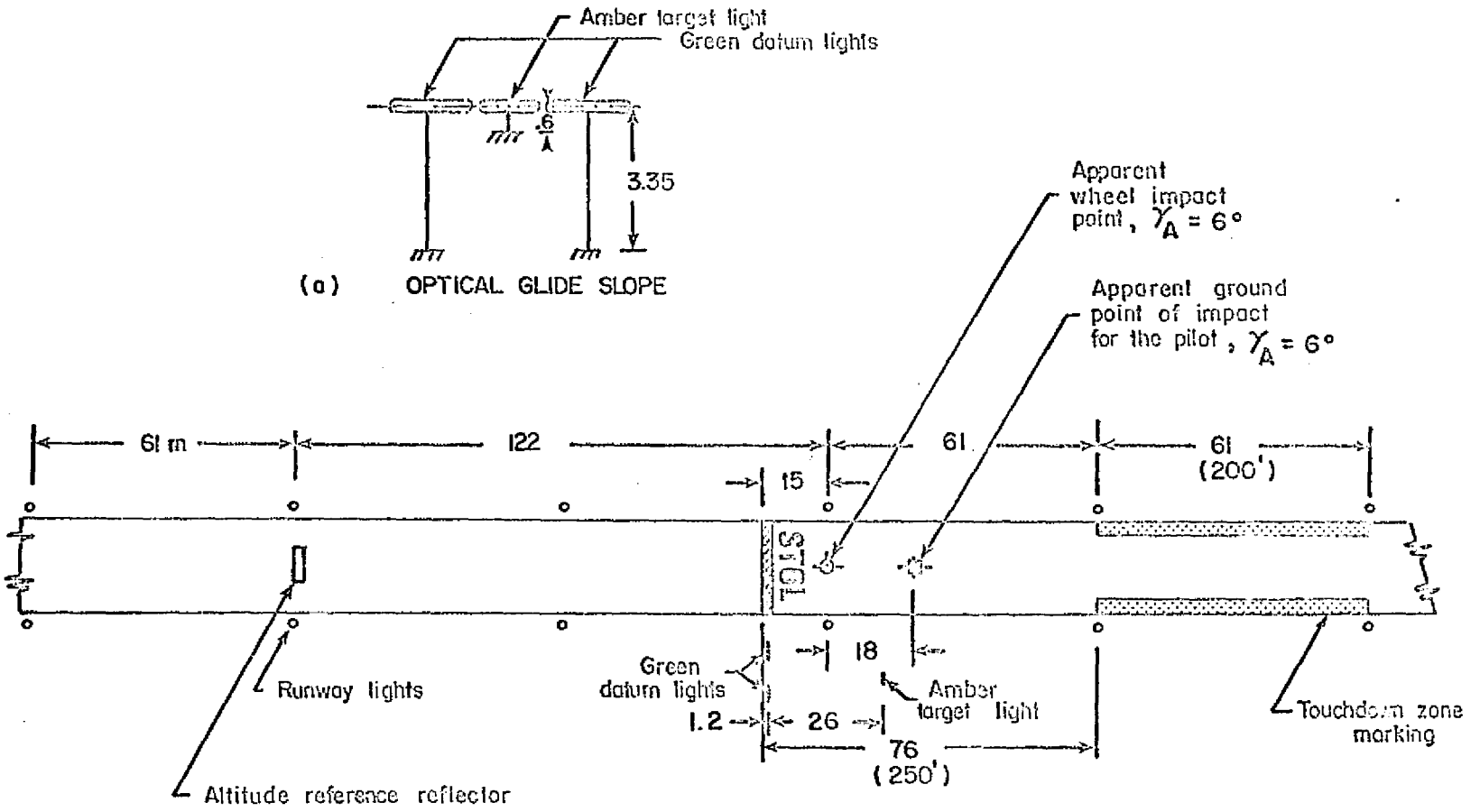

FIGURE 3. RUNWAY AND APPROACH GUIDANCE GEOMETRY

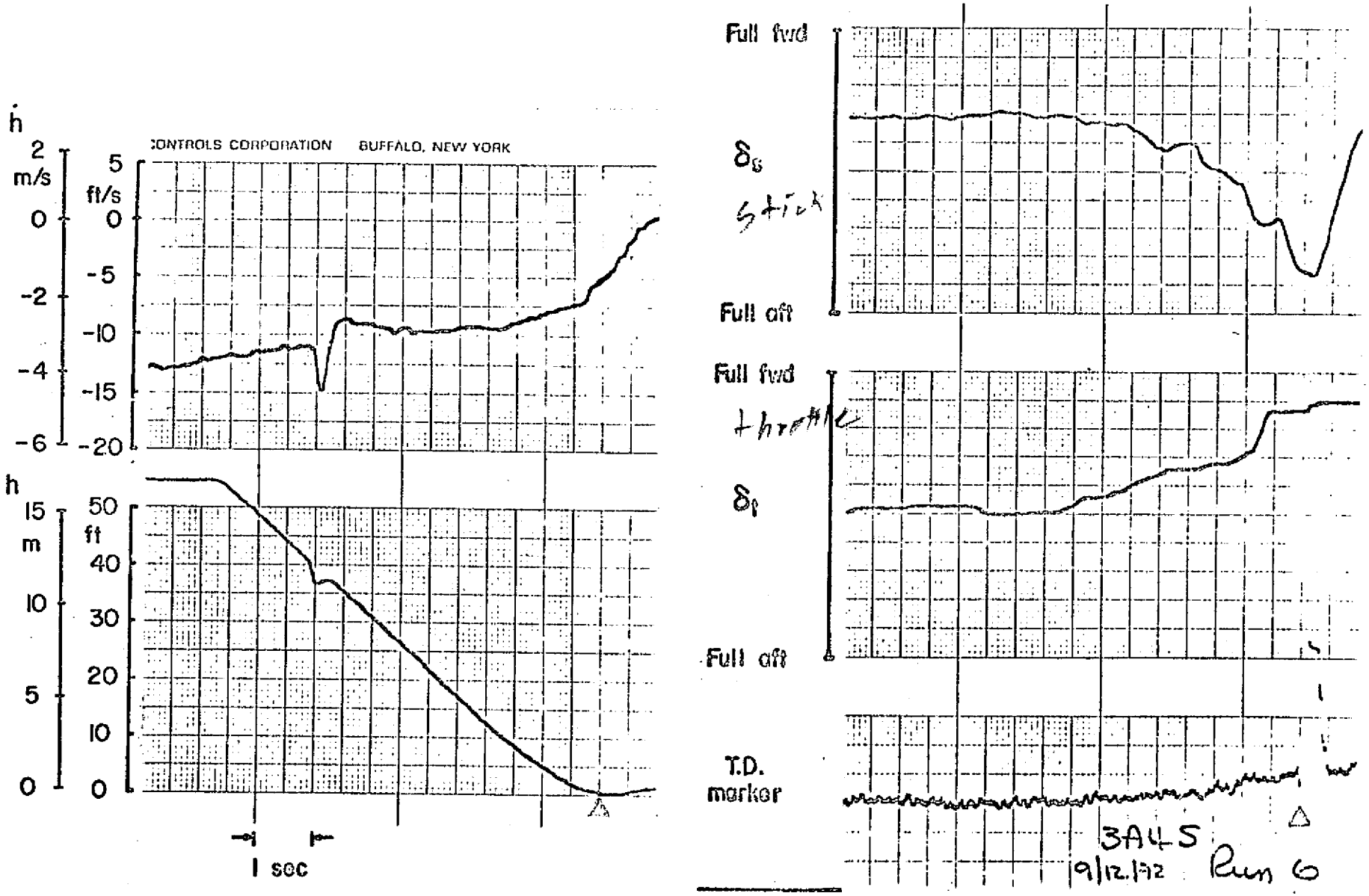

FIGURE 4. SAMPLE LANDING TIME HISTORIES

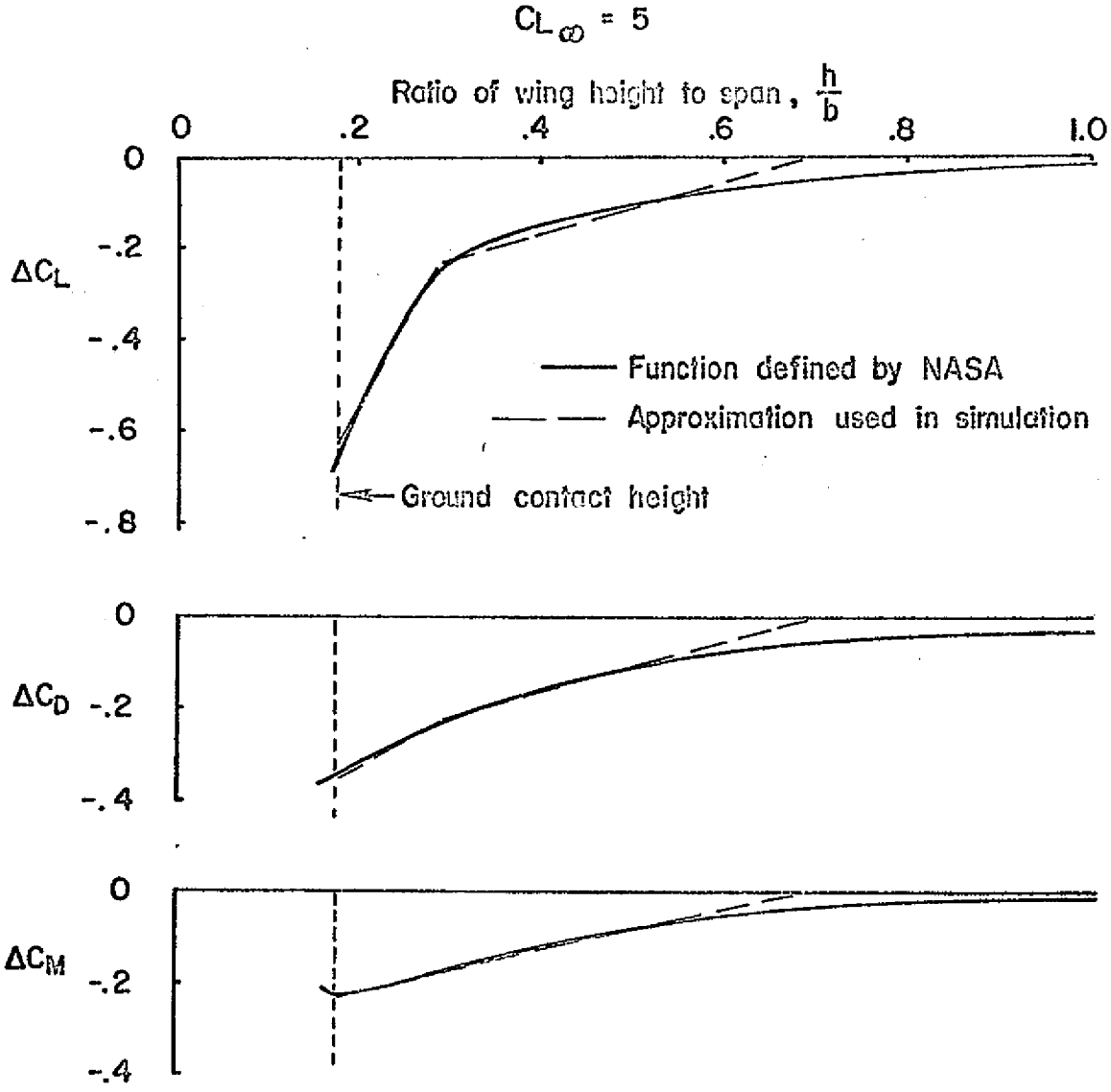

FIGURE 5. LIFT, DRAG, AND PITCHING MOMENT CHANGES IN GROUND EFFECT

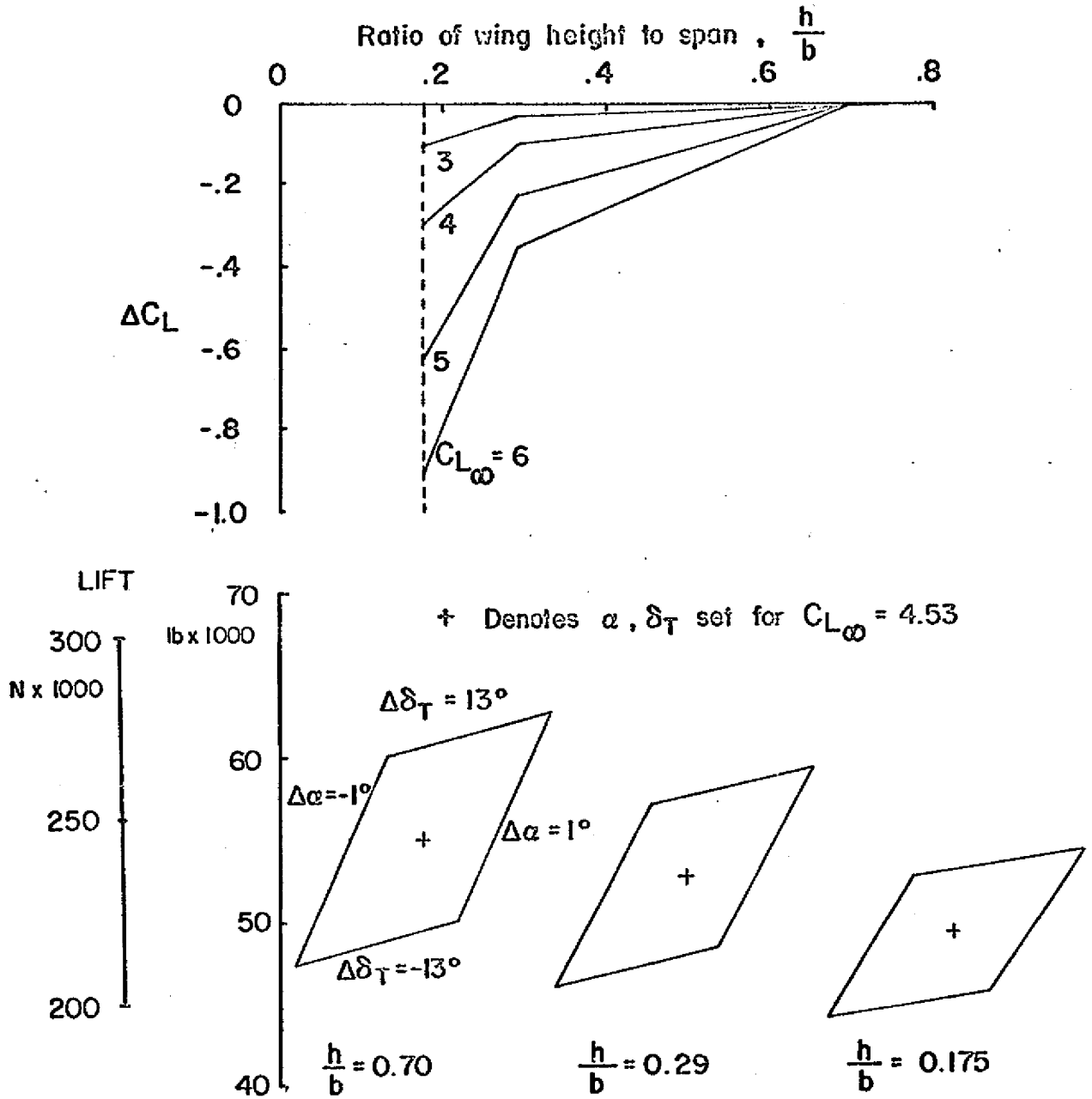

FIGURE 6. LIFT VARIATION WITH ALTITUDE, ANGLE OF ATTACK, AND THRUST

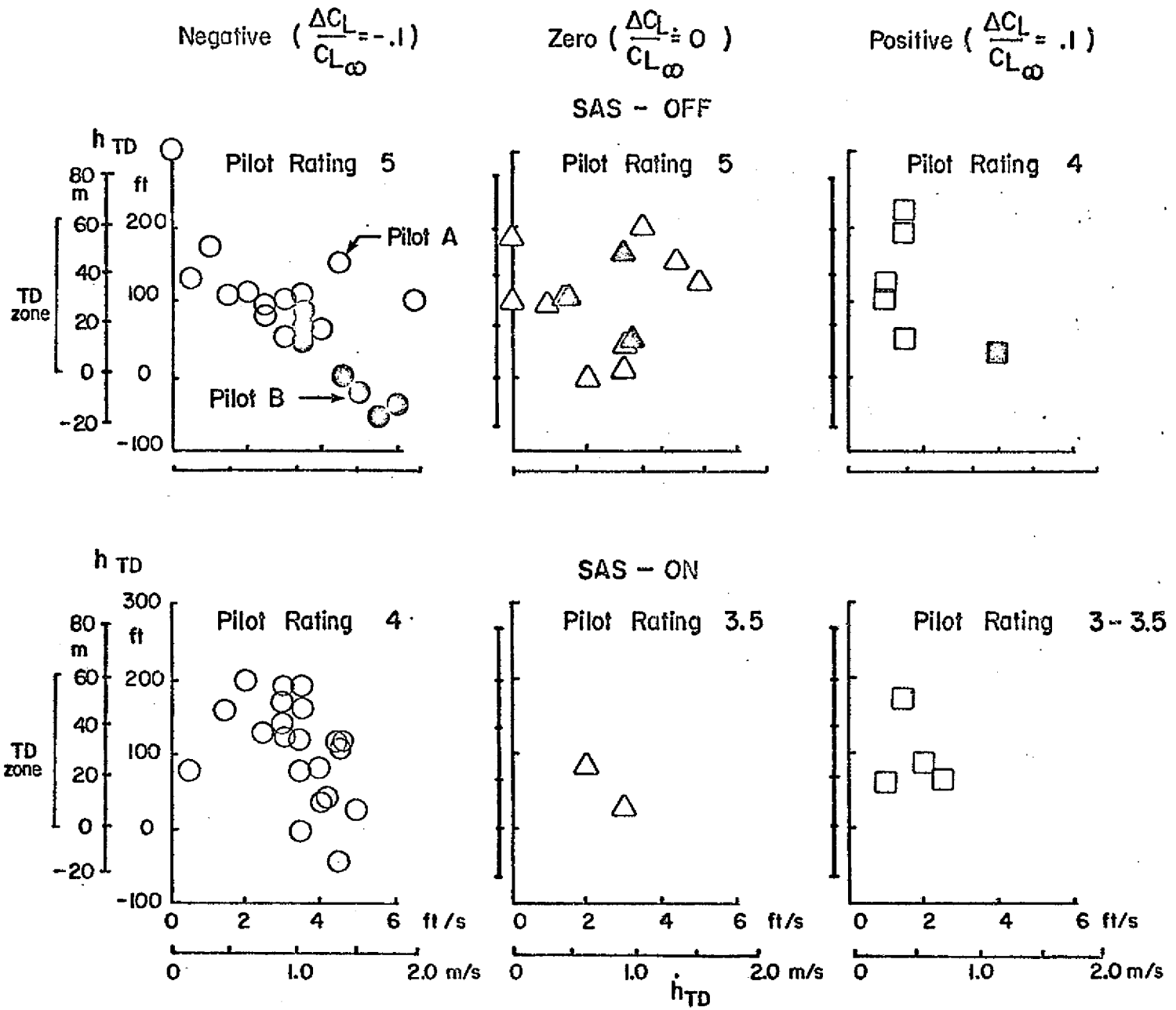

FIGURE 7. INFLUENCE OF GROUND EFFECT MAGNITUDE

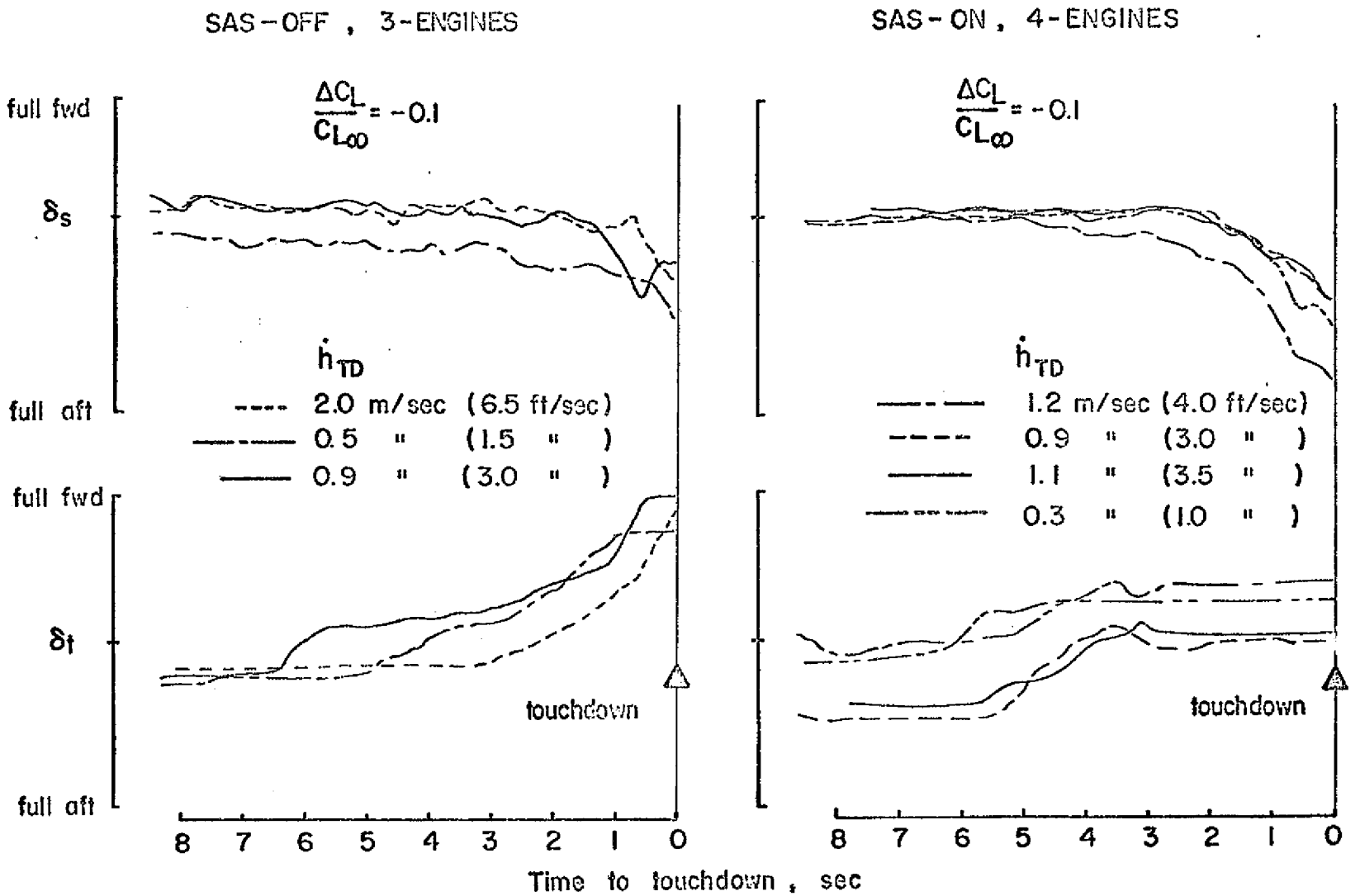

FIGURE 8. CONTROL INPUT TIME HISTORIES

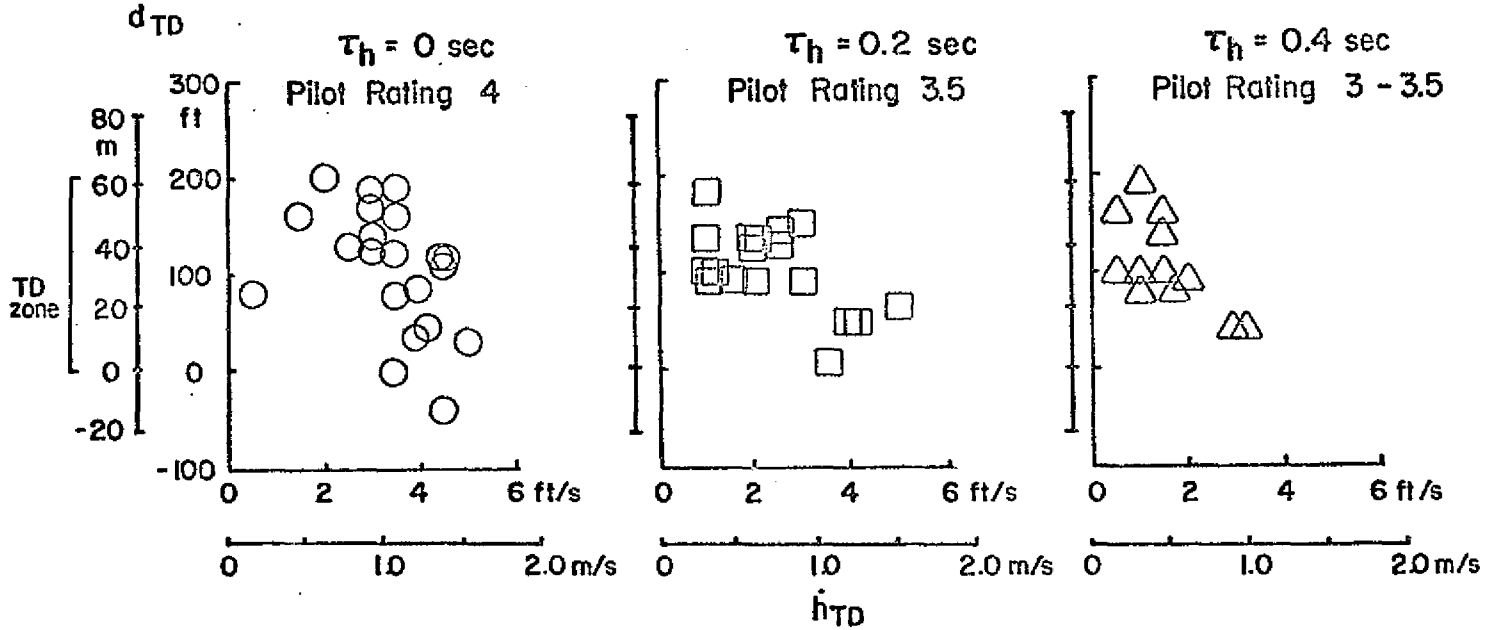

FIGURE 9. INFLUENCE OF GROUND EFFECT LAGS

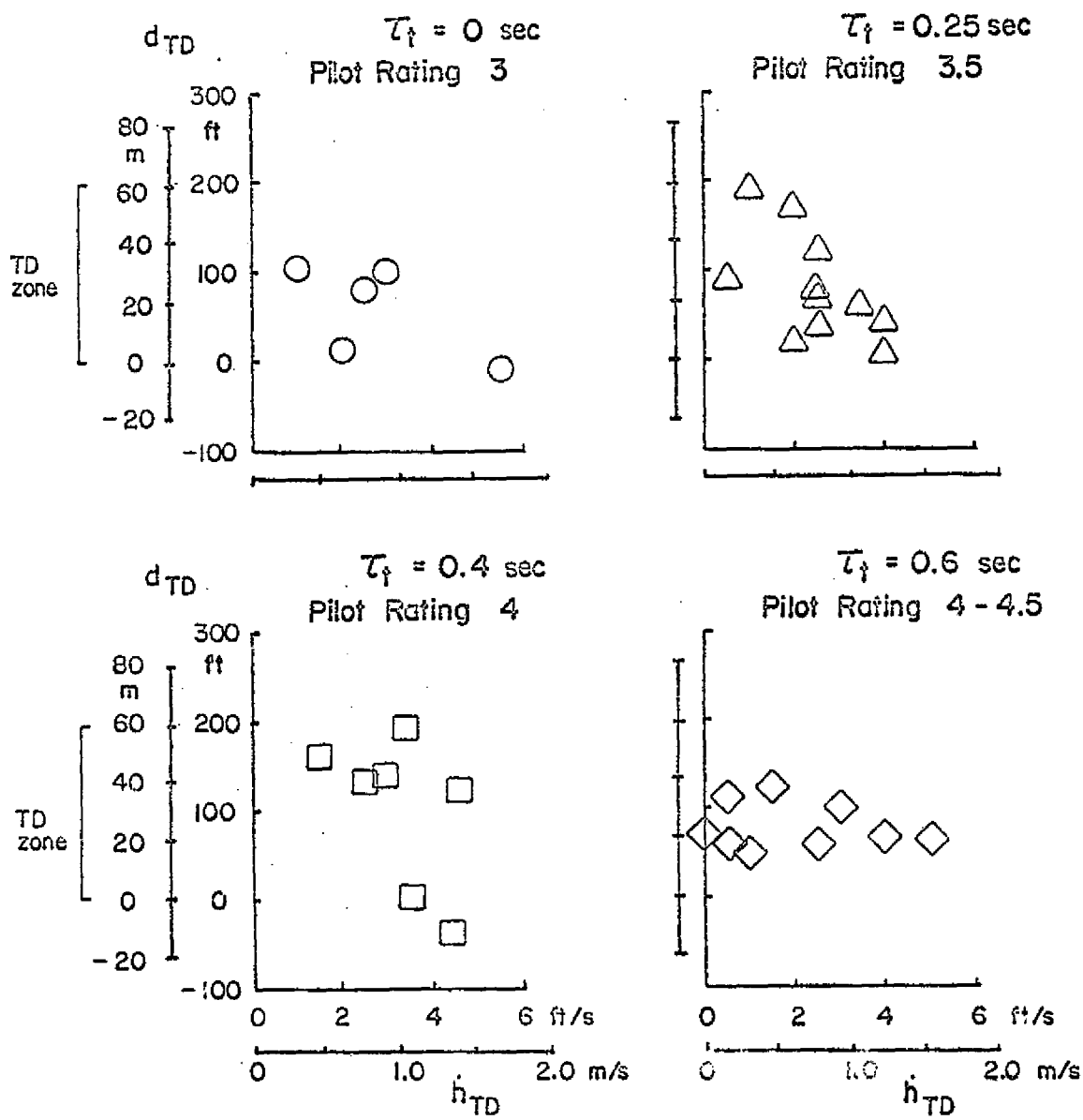

FIGURE 10. INFLUENCE OF THRUST RESPONSE LAGS

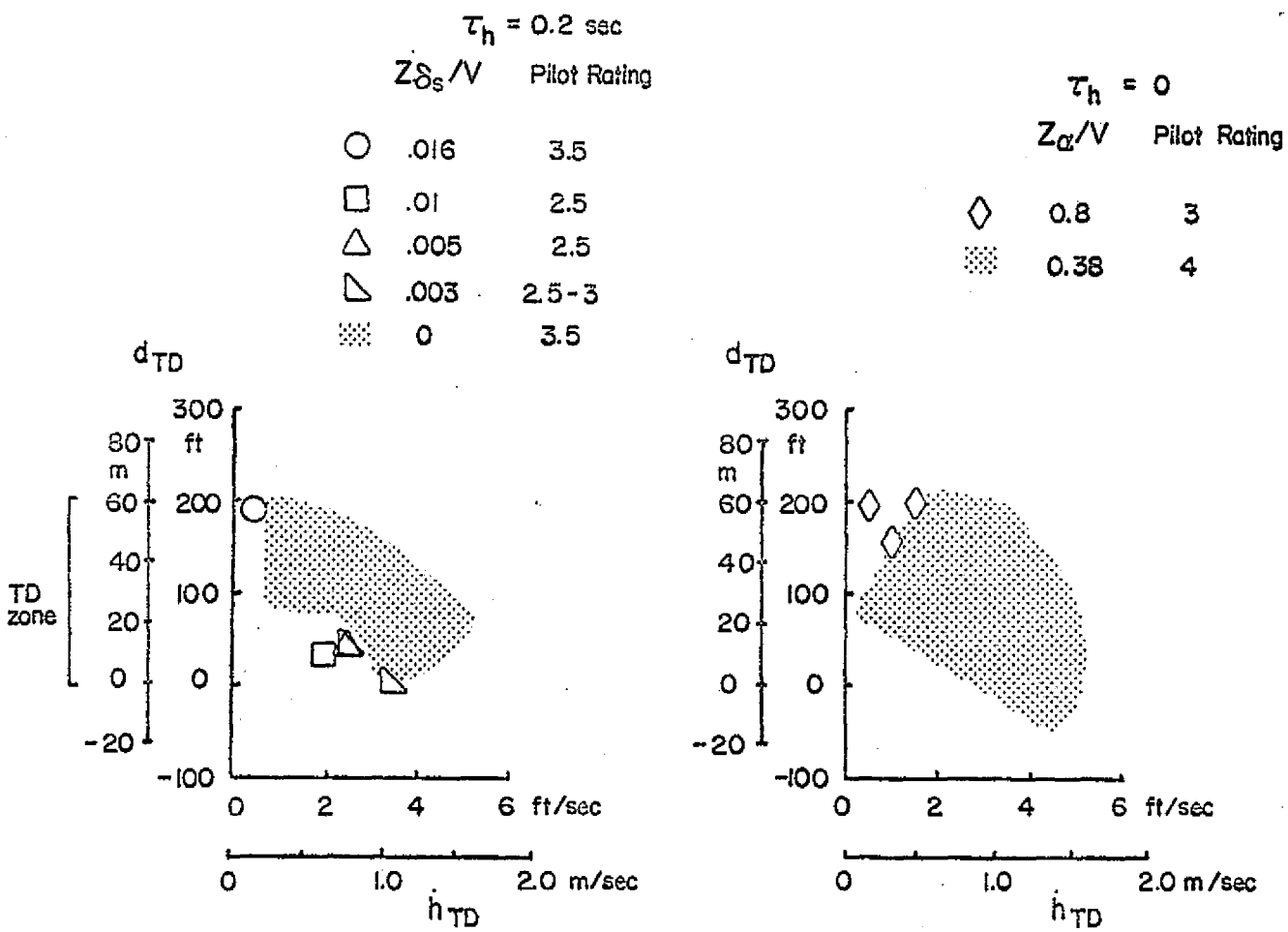

FIGURE 11. EFFECTS OF AUGMENTED LIFT RESPONSE

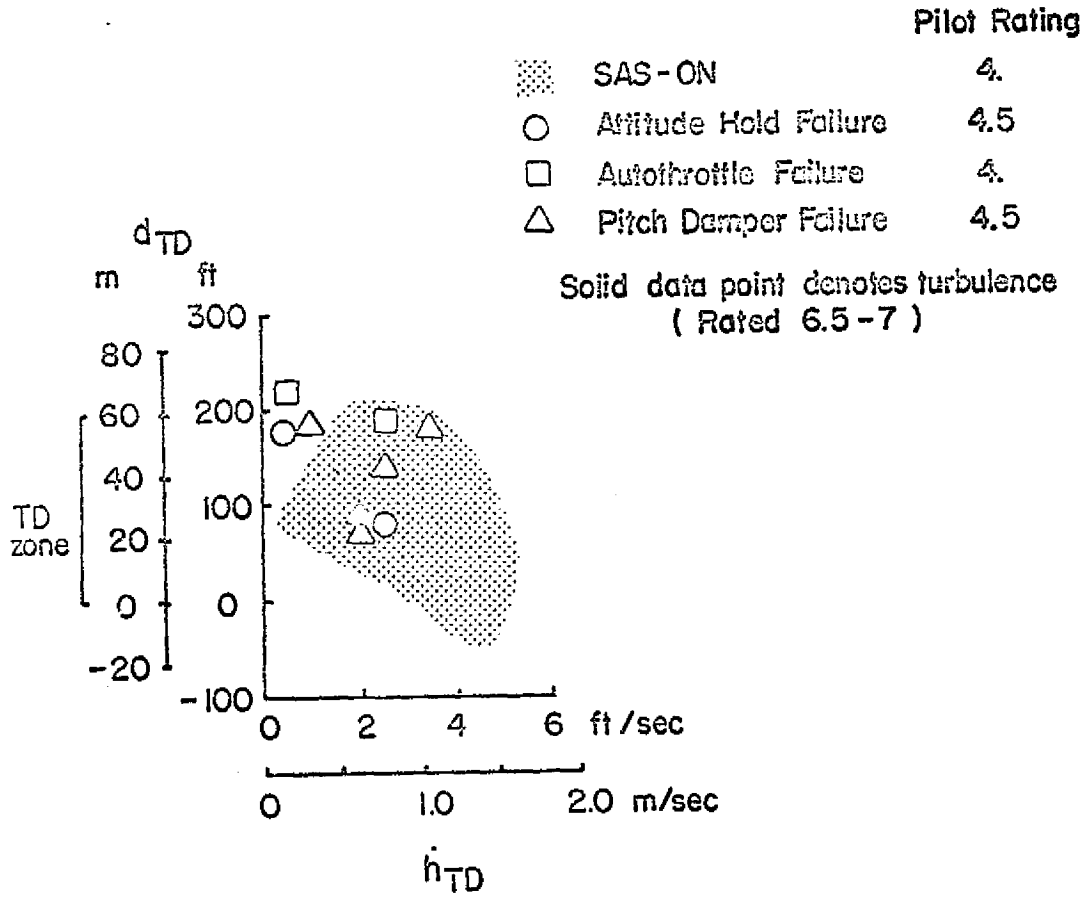

FIGURE 12. INFLUENCE OF SAS FAILURES

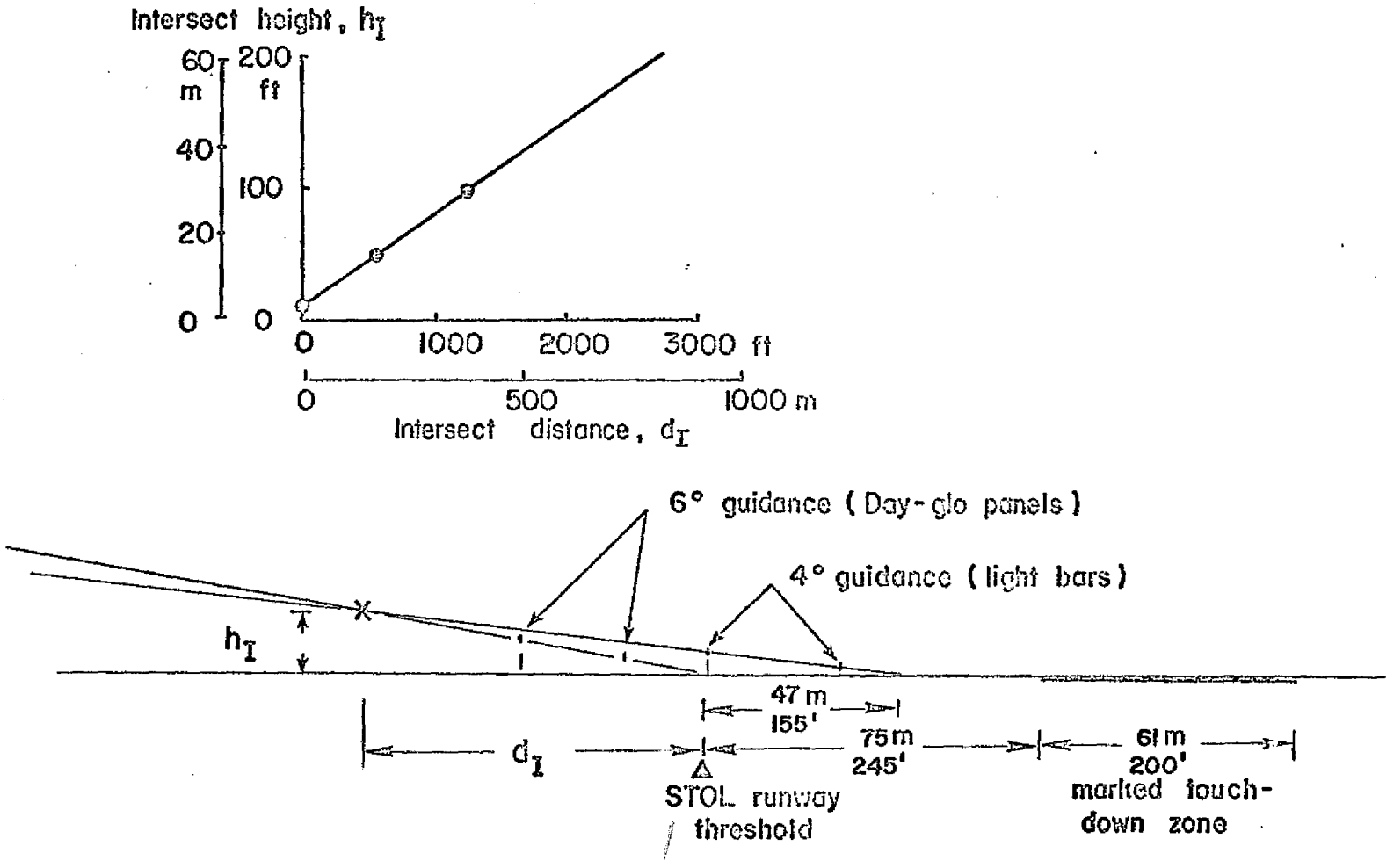

FIGURE 13. SEGMENTED APPROACH GEOMETRY

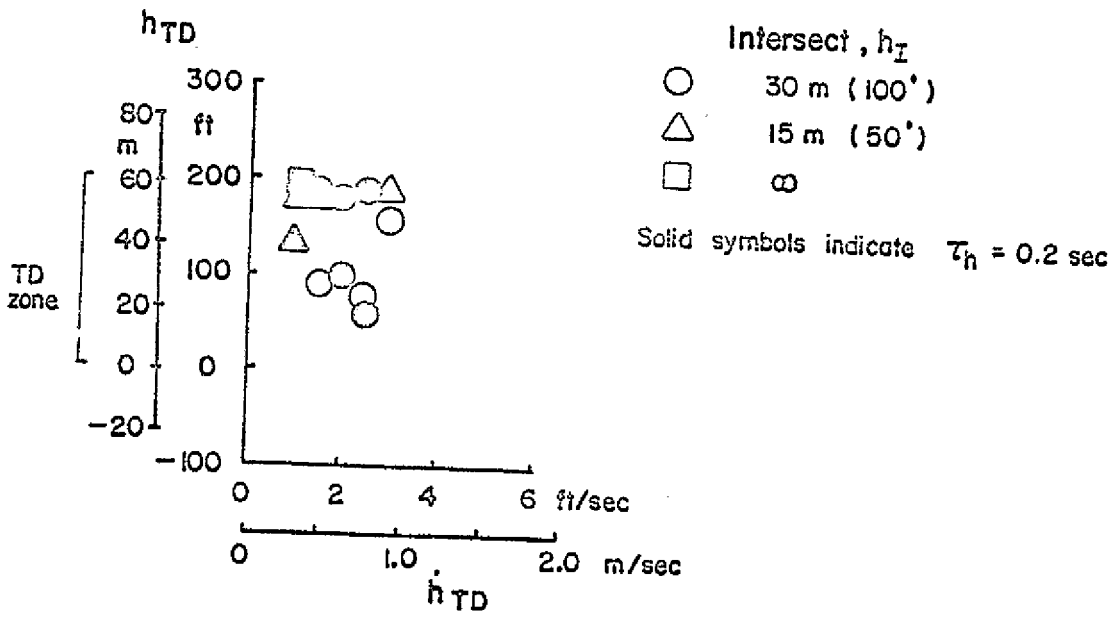

FIGURE 14. LANDING RESULTS WITH A SEGMENTED APPROACH

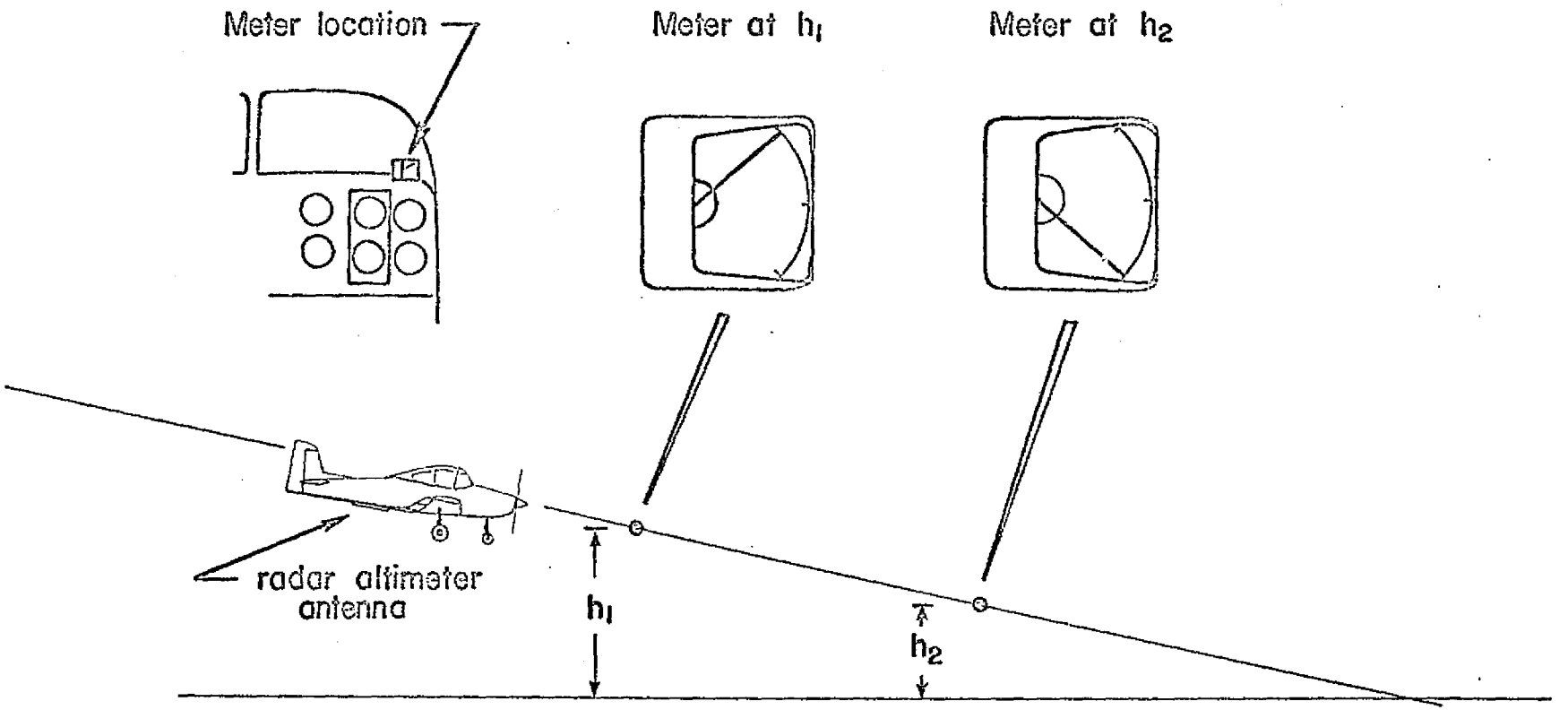

FIGURE 15. FLARE WARNING INSTRUMENT

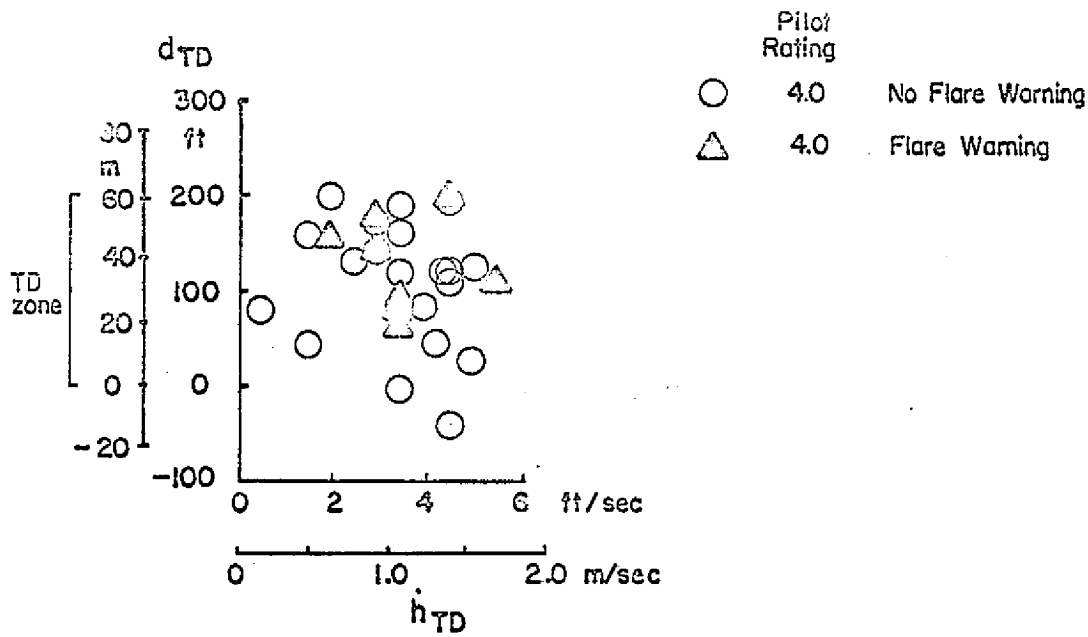

FIGURE 16. LANDING RESULTS WITH FLARE WARNING

APPENDIX C

NOTATION

C_L	lift coefficient
C_{L_∞}	lift coefficient out of ground effect
d_{TD}	touchdown point, ft, m
$d\gamma/du$	change of flight path with speed, thrust constant, deg/kt
g	acceleration due to gravity, ft/sec^2, m/sec^2
h	altitude, ft, m
$\dot{h}$	vertical velocity, ft/sec, m/sec
h_I	segmented glide slope intersect height, ft, m
I_x	roll moment of inertia, slug-ft^2, kg-m^2
I_y	pitch moment of inertia, slug-ft^2, kg-m^2
I_z	yaw moment of inertia, slug-ft^2, kg-m^2
IFR	instrument flight rules
L	rolling moment, ft-lb, N-m
L_β	dihedral effect, $\frac{1}{I_x}\frac{\partial L}{\partial \beta}$, rad/sec^2 per rad
L_p	roll damping derivative, $\frac{1}{I_x}\frac{\partial L}{\partial p}$, rad/sec^2 per rad/sec
L_r	roll due to yaw rate derivative, $\frac{1}{I_x}\frac{\partial L}{\partial r}$, rad/sec^2 per rad/sec
L_{δ_a}	roll control effectiveness, $\frac{1}{I_x}\frac{\partial L}{\partial \delta_a}$, rad/sec^2/in., rad/sec^2/cm

M	pitching moment, ft-lb, N-m
$M_{\dot{\theta}}$	pitch-rate damping, $\frac{1}{I_y}\frac{\partial M}{\partial \dot{\theta}}$, 1/ sec
M_u	pitch acceleration derivative due to speed, $\frac{1}{I_y}\frac{\partial M}{\partial u}$, rad/ sec^2 per ft/ sec, rad/ sec^2 per m/ sec
M_α	static stability derivative, $\frac{1}{I_y}\frac{\partial M}{\partial \alpha}$, rad/ sec^2/ rad
M_{δ_s}	pitch control effectiveness, $\frac{1}{I_y}\frac{\partial M}{\partial \delta_s}$, rad/ sec^2 per in., rad/ sec^2 per cm
m	aircraft mass, slug, kg
n	normal acceleration, g
N	subscript denoting Navion
N	yawing moment, ft-lb, N-m
N_β	directional stability derivative, $\frac{1}{I_z}\frac{\partial N}{\partial \beta}$, rad/ sec^2/ rad
N_r	yaw rate damping derivative, $\frac{1}{I_z}\frac{\partial N}{\partial r}$, rad/ sec^2 per rad/ sec
N_p	yaw due to roll rate derivative, $\frac{1}{I_z}\frac{\partial N}{\partial p}$, rad/ sec^2 per rad/ sec
N_{δ_r}	yaw control effectiveness, $\frac{1}{I_z}\frac{\partial N}{\partial \delta_a}$, rad/ sec^2/ in., rad/ sec^2/ cm
S	subscript denoting STOL airplane
SAS	stability augmentation system
u	airspeed perturbation, knots, ft/ sec, m/ sec or fore and aft gust velocity component
v	side gust component, ft/ sec, m/ sec

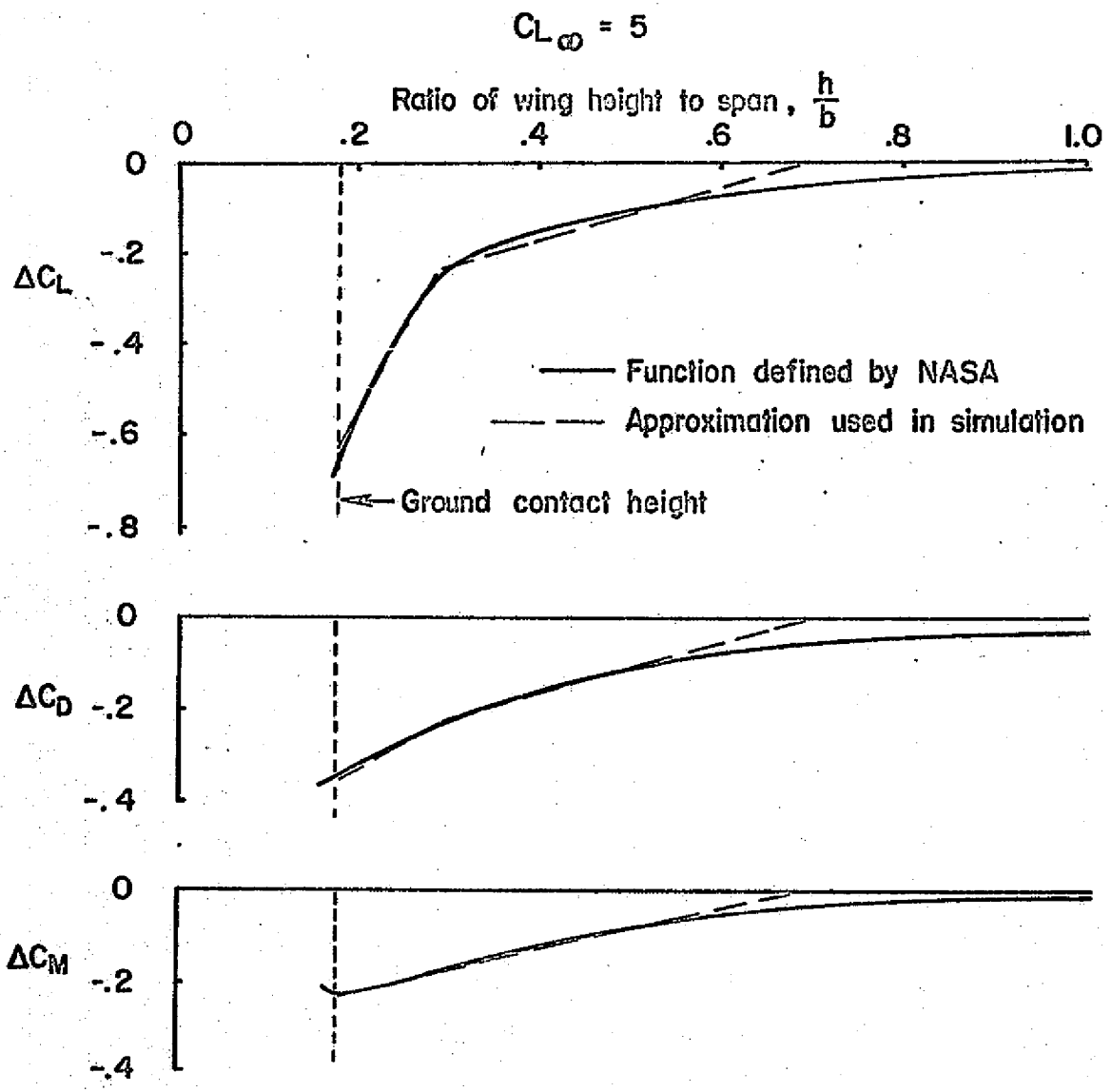

FIGURE 5. LIFT, DRAG, AND PITCHING MOMENT CHANGES IN GROUND EFFECT

V	airspeed, knots, ft/ sec, m/ sec
V_A	approach airspeed, knots, ft/ sec, m/ sec
VFR	visual flight rules
w	vertical gust component, ft/ sec, m/ sec
X	longitudinal force, lb, N
X_u	longitudinal acceleration derivative, $\frac{1}{m}\frac{\partial X}{\partial u}$, 1/ sec
X_α	longitudinal acceleration due to angle of attack, $\frac{1}{m}\frac{\partial X}{\partial \alpha}$, ft/ sec^2/ rad, m/ sec^2/ rad
Y	side force, lb, N
Y_β	side acceleration due to sideslip, $\frac{1}{m}\frac{\partial Y}{\partial \beta}$, ft/ sec^2/ rad, m/ sec^2/ rad
Z	vertical force, lb, N
Z_u	vertical acceleration due to speed, $\frac{1}{m}\frac{\partial Z}{\partial u}$, 1/ sec
Z_α	vertical acceleration due to angle of attack, $\frac{1}{m}\frac{\partial Z}{\partial \alpha}$, ft/ sec^2/ rad, m/ sec^2/ rad
Z_{δ_s}	lift due to control deflection, ft/ sec^2/ in., m/ sec^2/ cm
α	angle of attack, deg, rad
β	sideslip angle, deg. rad
γ	flight path angle, deg, rad
δ_a	roll control deflection, in., cm
δ_r	rudder pedal deflection, in., cm
δ_s	pitch stick deflection, in., cm

ζ_{sp}, ω_{sp}	damping ratio and natural frequency of the short period mode
ζ_{p}, ω_{p}	damping ratio and natural frequency of the phugoid mode
ζ_{θ}, ω_{θ}	damping ratio and natural frequency of the pitch response with attitude hold and pitch rate loops closed (attitude command SAS)
θ	pitch attitude, deg, rad
$\sigma_{(\ )}$	RMS gust velocity, ft/ sec, m/ sec
τ_{h}	time constant of ground effect lag, sec
τ_{t}	time constant of response to thrust command, sec
τ_{r}	roll mode time constant, sec
ω	frequency, rad/ sec